ORIGINAL ARTICLE

Feasible Dose Reduction in Routine Chest Computed Tomography Maintaining Constant Image Quality Using the Last Three Scanner Generations: From Filtered Back Projection to Sinogram-affirmed Iterative Reconstruction and Impact of the Novel Fully Integrated Detector Design Minimizing Electronic Noise

Lukas Ebner, Felix Knobloch, Adrian Huber, Julia Landau, Daniel Ott, Johannes T Heverhagen, Andreas Christe

Department of Diagnostic, Interventional and Pediatric Radiology, Inselspital, Bern University Hospital, Freiburgstrasse, Bern, Switzerland

Address for correspondence:
Dr. Lukas Ebner,
Department of Diagnostic, Interventional and Pediatric Radiology, Inselspital,
Bern University Hospital, Freiburgstrasse 10, 3006-CH Bern, Switzerland.
E-mail: Lukas.ebner@insel.ch

Access this article online	
Quick Response Code:	**Website:** www.clinicalimagingscience.org
	DOI: 10.4103/2156-7514.137826

ABSTRACT

Objective: The aim of the present study was to evaluate a dose reduction in contrast-enhanced chest computed tomography (CT) by comparing the three latest generations of Siemens CT scanners used in clinical practice. We analyzed the amount of radiation used with filtered back projection (FBP) and an iterative reconstruction (IR) algorithm to yield the same image quality. Furthermore, the influence on the radiation dose of the most recent integrated circuit detector (ICD; Stellar detector, Siemens Healthcare, Erlangen, Germany) was investigated. **Materials and Methods:** 136 Patients were included. Scan parameters were set to a thorax routine: SOMATOM Sensation 64 (FBP), SOMATOM Definition Flash (IR), and SOMATOM Definition Edge (ICD and IR). Tube current was set constantly to the reference level of 100 mA automated tube current modulation using reference milliamperes. Care kV was used on the Flash and Edge scanner, while tube potential was individually selected between 100 and 140 kVp by the medical technologists at the SOMATOM Sensation. Quality assessment was performed on soft-tissue kernel reconstruction. Dose was represented by the dose length product. **Results:** Dose-length product (DLP) with FBP for the average chest CT was 308 mGy*cm ± 99.6. In contrast, the DLP for the chest CT with IR algorithm was 196.8 mGy*cm ± 68.8 ($P = 0.0001$). Further decline in dose can be noted with IR and the ICD: DLP: 166.4 mGy*cm ± 54.5 ($P = 0.033$). The dose reduction compared

to FBP was 36.1% with IR and 45.6% with IR/ICD. Signal-to-noise ratio (SNR) was favorable in the aorta, bone, and soft tissue for IR/ICD in combination compared to FBP (the *P* values ranged from 0.003 to 0.048). Overall contrast-to-noise ratio (CNR) improved with declining DLP. **Conclusion:** The most recent technical developments, namely IR in combination with integrated circuit detectors, can significantly lower radiation dose in chest CT examinations.

Key words: Dose reduction, low-dose CT, stellar detector

INTRODUCTION

Since the introduction of computed tomography (CT) in clinical practice in the late 1970s, dose reduction has been a major concern for radiologists and their patients.[1,2] Over the last few decades, spiral CT, cardiac imaging, perfusion techniques, high-pitch CT, and dual-energy CT have been introduced to clinical practice, increasing the overall amount of radiation applied.[3,4] In contrast, a multitude of dose reduction methods have been developed on the hardware side, such as dose modulation along the *x*-, *y*-, and *z*-axes.[5-8] Shielding[9-14] demonstrates a further major step in manufacturer-dependent radiation protection. A recent vast improvement toward ultra-low-dose CT was the implementation of iterative reconstruction (IR) algorithms in the most recent scanner generations. IR has the potential to lower the amount of radiation applied significantly and to maintain the radiation at a constant minimum.[15,16] The introduction of the most recent fully integrated circuit detector (ICD) geometry, realized in the Stellar detectors by Siemens (Erlangen, Germany), demonstrated initial promising potential to reduce the radiation further[17] by minimizing electronic noise. To lower the image noise, this new detector assembly combines the electronics and the photodiode into a single unit. Additionally, a major concern in dose reduction has been the preservation of diagnostic image quality, measured by noise, the signal-to-noise ratio (SNR), and the contrast-to-noise ratio (CNR).[18-20] The previous data have suggested that diagnostic image quality could be maintained while concurrently lowering the radiation dose, by adopting the recent technologies mentioned above.[21,22] We hypothesized that the current implementation of an iterative algorithm and the launch of the ICD geometry would result in a sustainable dose reduction that would preserve the diagnostic image quality. We compared 150 standard chest CTs, from clinical routines that were acquired with the standard Siemens scan parameter presettings, with an intravenous contrast application on a Siemens Sensation scanner with filtered back projection (FBP), the most recent Siemens Definition Flash scanner with IR and the Siemens Edge CT scanner, which was also equipped with IR and ICD.

Furthermore, we compared the median radiation doses. The image quality was also assessed during the read-out process by determining SNR and CNR measurements.

MATERIALS AND METHODS

This study was approved by the local ethics committee. Because this study was conducted retrospectively, written informed consent from the patients was waived by the committee. A total of 150 consecutive patients from our clinical practice were enrolled in this retrospective investigation. Fifty patients were scanned using FBP, 50 patients were examined applying iterative image reconstruction (IR), and 50 patients were scanned with ICD using IR, which were identified from the patient set.

The patients were selected by applying the inclusion criteria outlined below:
A standard chest CT, with arterial phase after intravenous contrast media injection, must have been performed on all of the patients, using the same standard preset scan parameters as outlined below. All the scans were required to exhibit diagnostic image quality. Patients with artifacts that resulted in non-diagnostic data sets were excluded from the study population. Attention was paid to foreign bodies (i.e. metal or prostheses); therefore, there were no beam-hardening artifacts in the scan range that could have caused a large increase in the radiation dose. Native scans of the chest or multiphase acquisitions were excluded.

A total of 150 patients (98 men, 52 women) were retrospectively enrolled in this study. After applying the inclusion criteria, 136 patients remained in the study population, which consisted of 91 male and 46 female patients. Fourteen patients (eight men, six women) were excluded. In one case, the contrast medium was injected extravascularly. In 12 cases, additional scans with late enhancements were ordered. One patient received additional expiratory scans for the assessment of air trapping, which resulted in the patient's exclusion from the study population. The case mix in all of the groups consisted of patients who were examined for oncological staging, infectious disease, or trauma. After applying the inclusion criteria, the patients (*n*) remaining in each

subgroup (FBP, IR, IR/ICD) were as follows: $n = 48$ for FBP, $n = 44$ for IR, and $n = 44$ for IR/ICD. The mean patient age in the study group at the time of the examination was 51 years (range 8-94 years).

The scan parameters were identical to the manufacturer's standard presettings for a thorax routine: SOMATOM Sensation 64 (24 × 1.2 mm, pitch 0.8, slice thickness 1.5 mm, FBP); SOMATOM Definition Flash (128 × 0.6 mm, pitch 0.6, slice thickness 1 mm, IR); and SOMATOM Definition Edge (128 × 0.6 mm, pitch 0.6, slice thickness 1 mm, ICD and IR), all by Siemens (Erlangen, Germany). Eighty milliliters of intravenous contrast medium (Iopamiro 300, Bracco Suisse SA, Manno) was injected (injection rate: 3 ml/s). Saline flush of 20 ml was applied. Bolus-triggered scan timing was used on all three scanner types. Aortic threshold for triggering was 100 Hounsfield units (HU). In addition, 5 mm axial slice reconstructions were performed on all three scanners. The standard tube potential (kVp) and tube current (mA) settings for the Siemens routine protocol for the thorax (adapted vendor standard) were maintained constantly on all the scanner generations. An automated tube current modulation (Care Dose®; Siemens, Erlangen, Germany), using reference mA (ref. mA) to individually adapt the radiation exposure to the patient size, was implemented on all three of the CT scanners. In addition, Care kV was used on the Flash scanner and the SOMATOM Definition Edge. Tube potential on the Sensation scanner was chosen individually for each patient depending on patient size. The measurements for quality assessment were performed on a soft-tissue kernel reconstruction (B30f, I31f). The standard reconstructions also included a lung kernel reconstruction (B70f, I70f) and coronal and sagittal projections. All the image evaluations were performed on the 5 mm axial slice reconstructions. For the iterative image reconstruction on the Flash and Edge scanners, an iteration level of three was specified in all the cases. An iteration level of three provided a reasonable trade-off between a low radiation dose and image noise.[23] All the patients were scanned in supine position, starting at the superior thoracic inlet and covering the entire lung to the lung bases (including the whole lung parenchyma). The scans were performed with deep forced inspiration. The dose used in conjunction with every CT study was listed by the manufacturer in a dose protocol and was represented by the dose-length product (DLP, mGy*cm) provided by the scanners for a 32-cm-diameter phantom for each scan. In addition, the computed tomography dose index per volume (CTDI Vol.) was provided.

For every patient, the chest volume was calculated retrospectively using the formula for cylindrical objects:

(sagittal diameter/2) × (transverse diameter/2) × π × scan length.

Image analysis

To evaluate the image quality for each scanner generation, one reader (with 4 years of experience in chest CT imaging) performed the assessment of the noise, the background noise, and the SNR, as well as the CNR, which represented the overall image quality. The analysis was performed on a Picture Archiving and Communication System (PACS; EasyVision Sectra, Sweden). First, the DLP (mGy × cm) and computed tomography dose index in the scan volume (CTDI Vol.) were retrospectively retrieved from the PACS system for each study and were collected in a standard Microsoft Excel (Windows©) scoring sheet. For the assessment of the SNR, CNR, and the background noise, we measured the signal represented by the density in HU and the standard deviation of the HU (noise) in a region of interest (ROI) with a standardized diameter of 1 cm (0.79 cm^2). The ROIs were consistently placed in the following locations on a transverse slide, immediately above the diaphragm on 5 mm axial slice reconstructions, using a soft-tissue kernel (B31f; I31f). The first ROI was outlined in the air outside of the body and anterior to the sternum for the assessment of background noise. Another ROI was placed in the middle of the aorta at the same level. Further ROIs were outlined in the middle of a vertebral body at the same level (carefully sparing the intervertebral space) and in the paraspinal muscles (M. erector spinae). Measurements were recorded for air, soft tissue, the aorta, and bones in the soft-tissue kernel. The SNR was calculated for all the recorded parameters by dividing the signal intensity (SI) of the soft tissue by the background noise:

$$SNR = \frac{SI \ (soft \ tissue \ in \ HU)}{SD \ (background \ noise)}$$

We calculated the CNR for the aorta and lung. The CNR in the aorta was defined as the difference between the signals (HU) in the aorta and soft tissue divided by the soft tissue noise in HU measured in the aorta above the diaphragm.

$$CNR \ (aorta) = \frac{(SI \ (aorta) - SI \ (soft \ tissue \ in \ HU))}{HU \ (soft \ tissue \ noise)}$$

In contrast, the CNR of the lung was represented by the difference between the signals of the soft tissue and air, divided by the soft tissue noise.

Statistical analysis

The distribution of the presented, quantitative, rational data was assessed using D'Agostino's K-squared method (a.k.a.

the D'Agostino-Pearson test).[24] Assuming a skewed distribution of the data, this test established whether the data were derived from a normally distributed population. The results were verified with the Shapiro-Francia test for normality, which indicates a predominantly non-normal data distribution. For the analysis of two unpaired, independent data sets, a non-parametric Mann-Whitney test for two-sided, independent samples was applied. $P < 0.05$ was considered statistically significant. The data were collected using Microsoft Excel (Microsoft Office® 2010). The statistical analysis was performed using MedCalc®, version 7.6.0.0 (MedCalc Software, Mariakerke, Belgium), and Microsoft Excel® 2010. The scatter plot of image quality to radiation dose for each scanner generation was obtained.

RESULTS

Radiation dose

The radiation dose decreased with every technical advance from FBP to IR and further with IR/ICD [Table 1]. The DLP with FBP for the average chest CT was 308 mGy*cm ± 99.6. In contrast, the DLP for the chest CT examination with an IR algorithm was 196.7 mGy*cm ± 68.8 (FBP vs. IR: $P < 0.0001$). A further decline in the radiation dose was observed with the combination of IR and ICD: DLP was 167.5 mGy*cm ± 54.5 (IR vs. IR/ICD: $P < 0.0332$) [Figure 1]. Corresponding with the reduction in the DLP, the CTDI Vol. decreased from 7.8 ± 2.5 (FBP) to 5.4 ± 2.0 (IR) and finally to 4.5 ± 1.5 (IR/ICD). The P values for these data were also demonstrated to be statistically significant [Table 1]. In other words, the dose reduction, compared to FBP, was 36.1% with IR and 45.6% with IR/ICD.

Image quality

Table 2 summarizes the measured values for the signal and noise in air, aorta, bone, and soft tissue for each of the different CT scanners. The signal in bone was significantly higher using IR combined with ICD than using FBP ($P < 0.006$). The improvement of the bone signal from FBP to IR alone was not significant. The noise in soft tissue was significantly lower with IR/ICD than with FBP ($P < 0.001$).

SNR values of the aorta, bone, and soft tissue improved significantly switching from FBP on the SOMATOM Sensation scanner to IR/ICD in combination (P values ranging from 0.017 to 0.003) [Table 3]. For the assessment of image quality, Table 3 displays the SNR and CNR calculations for air, bone, aorta, and soft tissue. The total image quality based on average SNR measurements increased (ΔSNR FBP to IR/ICD: $P < 0.003$). There was no remarkable enhancement of CNR in moving from FBP to IR [Table 3]. CNR in the aorta was 11.6 ± 4.4, 12.8 ± 6.2, and 14.1 ± 6.9 for FBP, IR, and IR/ICD, respectively, representing favorable results for the IR/ICD combination. The CNR was 79.2 ± 43.9, 82.3 ± 50.4, and 61.5 ± 41.9 for FBP, IR, and IR/ICD, respectively [Table 3 and Figure 2]. CNR in relation to DLP and scanner type is displayed in Figure 3. Favorable CNR–DLP relation can be observed for the IR/ICD curve.

The mean chest volume of the patients in the three study groups did not differ significantly ($P = 0.36$-0.67): The mean body volume of the first patient group (SOMATOM Sensation) was 21.33 dm^3 ± 7.78 standard deviations (SDs), median = 21.28; the mean body volume of the second group (Flash, IR) was 23.84 dm^3 ± 6.66 (median = 23.34); in the third group (Edge, IR, and ICD), the chest volume was 20.09 dm^3 ± 5.88 (median = 19.63).
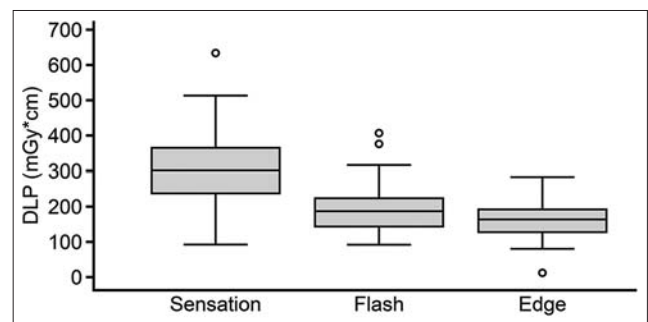

Figure 1: Box plot diagram of the dose distribution with FBP (Sens = sensation), Flash (IR), and Edge (IR/ICD). The dose represented by the DLP (in mGy*cm) declines with every technical advance.

Table 1: Dose reduction with IR and IR/ICD compared to FBP. Every step in the reduction is significant

	DLP	Dose reduction compared to FBP in %	P values
FBP	308.1		
IR	196.7	36.1	<0.0001
IR/ICD	167.5	45.6	<0.0001

IR: Iterative reconstruction, ICD: Integrated circuit detector, FBP: Filtered back projection

Table 2: Signal and noise calculations for filtered back projection, iterative reconstruction, and IR/ICD detector

		Air	Noise air	Aorta	Noise aorta	Bone	Noise bone	Soft tissue	Noise ST
FBP	Signal	−991.8±13.1	21.4±18.1	250.9±68.7	20.5±12.0	169.6±60.4	47.0±29.4	39.4±11.5	17.0±4.6
	P (1 vs. 3)	(<0.0001)	(<0.070)	(<0.190)	(<0.0001)	(<0.006)	(<0.150)	(<0.177)	(<0.001)
IR	Signal	−984.6±19.0	24.9±27.5	232.1±8.0	15.1±3.6	180.6±49.1	39.6±15.7	46.2±12.0	14.5±2.9
	P (1 vs. 2)	(<0.075)	(<0.777)	(<0.250)	(<0.0001)	(<0.198)	(<0.244)	(<0.002)	(<0.002)
IR and ICD	Signal	−981.0±14.3	26.9±8.4	228.1±75.1	13.7±3.1	206.1±70.1	40.8±20.7	42.7±11.3	15.1±6.5
	P (2 vs. 3)	(P<0.015)	(<0.084)	(<0.652)	(<0.077)	(<0.083)	(<0.838)	(<0.053)	(<0.392)

Signal: Hounsfield units, ST: Soft tissue, IR: Iterative reconstruction, ICD: Integrated circuit detector, FBP: Filtered back projection

Table 3: SNR and CNR measurements for FBP, IR, and IR/ICD

		SNR aorta	SNR bone	SNR ST	CNR aorta	CNR air
FBP	P (1 vs. 3)	13.8 ± 5.1 (0.017)	4.2 ± 2.0 (0.003)	2.8 ± 2.1 (0.018)	11.6 ± 4.4 (0.062)	79.2 ± 43.9 (0.069)
IR	P (1 vs. 2)	16.1 ± 6.7 (0.188)	5.0 ± 1.9 (0.040)	3.4 ± 1.3 (0.001)	12.8 ± 6.2 (0.700)	82.3 ± 50.4 (0.731)
IR/ICD	P (2 vs. 3)	17.5 ± 7.4 (0.295)	5.8 ± 2.5 (0.200)	3.2 ± 1.4 (0.301)	14.1 ± 6.9 (0.265)	61.5 ± 41.9 (0.072)

Signal: Hounsfield units, ST: Soft tissue, IR: Iterative reconstruction, ICD: Integrated circuit detector, FBP: Filtered back projection, SNR: Signal-to-noise ratio, CNR: Contrast-to-noise ratio
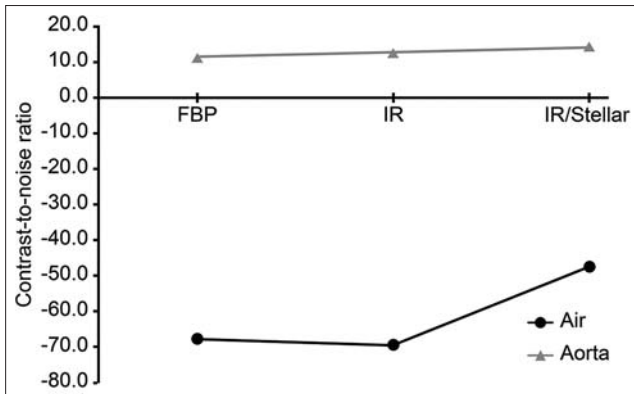

Figure 2: CNR in air and the aorta with the three scanners. The CNR in the aorta is constantly rising. Only the CNR in air exhibits a reduction with IR.

Figure 3: Scatter plot of the CNR/DLP relationship. Potential trend fitting curves are drawn for every scanner. The fitting curves indicate the mean distribution of CNR-DLP relationship for the separate data sets. Comparing the curves, the IR/ICD combination exhibits favorable CNR maintaining minimal DLP. IR and FBP trend curves show almost similar CNR, but DLP is significantly higher utilizing FBP.

DISCUSSION

Our findings clearly support the assumption that the most recent technical developments, namely IR in combination with an ICD design, could significantly lower the radiation dose burden for patients undergoing standard chest CT examinations. This finding was true even with the standard protocol settings from the manufacturer. The newer technology allowed for a lower tube potential, thus explaining the higher bone signal due to the increased photo effect of radiation at the lower tube potential levels.

In our study, we primarily investigated the feasibility of a dose reduction in chest CT by implementing the most recent software and hardware available at the time. On the software side, IR allows low-dose examinations. The radiation savings with the use of IR have been well-documented in the recent literature.[25] The availability of faster hardware components that reduce computing times has resulted in the standardized implementation of IR, especially with the latest CT scanner generation.[26] The possible dose reduction, in comparison with FBP, is evident and is supported by the present data, retrieved from clinical routines performed on this study population. On the hardware side of CT manufacturing, the minimization of electronic noise has been realized with the ICD by Siemens. Assuming that the noise increases with the distance between the photodiode and the chip, the logical approach to overcome this source of noise is to decrease this distance and to fully integrate the entire electronic component directly into the detector unit. Some initial studies have also demonstrated the possibility of minimizing the radiation
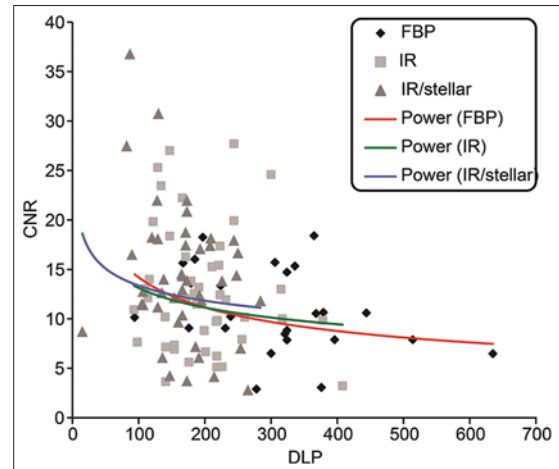
dose by implementing IR and ICD in the most recent CT scanner generation by Siemens Healthcare (Erlangen, Germany).[17]

Every step in technical improvement resulted in a significant radiation dose reduction, from FBP to IR and from IR to IR/ICD [Table 1] ($P < 0.0001$). As our results demonstrate, the possible radiation dose reduction on the software side was approximately 36% in changing from FBP to IR ($P < 0.0001$). Pontana et al., demonstrated almost the same dose reduction in their study, which compared IR and FBP in chest CT exams.[16] Additionally, using three steps of iteration, Pontana achieved a dose reduction of 35%. Further enhancement in radiation dose reduction obtained by implementing the integrated detector design and changing from the use of FBP to that of an IR/ICD detector was 45.6% ($P < 0.0001$), indicating that a further reduction of 9.4% from IR to IR/ICD ($P < 0.033$) was possible with a more effective detector design. These findings are in accordance with the results published by Christe et al., in a phantom-based setting. Implementing iterative reconstruction technique along with the ICD (Stellar detector by Siemens), a dose reduction between 27% and 70% was feasible in this phantom study.[27]

As indicated by the present data, the most evident reduction in dosage was achieved, however, when using IR in contrast to FBP ($P < 0.0001$). This major step in dose

reduction could be explained by the higher dose efficiency of iterative calculations and by the recent methods for accelerating statistical reconstruction.[28]

Not only was the dose reduction between the scanners evident, but also there was an increase in the image quality of the routine clinical CT images as a side effect. At least the radiological parameters of the signal to contrast and noise improved in soft tissues, the aorta, and bone (further studies are required to investigate the other physical parameters of image quality, such as spatial resolution and Z-sensitivity). Nevertheless, regardless of the tissue for which the SNR and CNR were calculated, these parameters increased (aorta, bone, or soft tissue). In fact, there is little use in calculating SNR of air/lung since the more negative these values get, the better it is for the radiologists (ideally, air should present with no signal). Therefore, SNR in the lung is worse for IR/ICD, which could influence the detection of ground-glass opacities to the worse. More importantly, the CNR does not vary significantly between the different scanner types, which are more relevant for disease detection. With SNR and CNR representing image quality, the present data indicated that the overall image quality increased as the dosage concurrently declined. A further dose reduction would therefore be possible if the improvement in image quality was sacrificed for radiation protection. Studies have demonstrated that a loss of image quality due to lower radiation levels did not automatically result in the loss of the diagnostic image quality.[29] Kalra et al., used this effect in their study investigating the sensitivity and specificity of abdominal CT, using IR in ultra-low-dose CT. They were able to conclude that a dose reduction of up to 74% was feasible, while conserving diagnostic image quality, with even less noise than in FBP.[30]

The signal represented in HU increased in bone and soft tissue with IR/ICD compared to FBP. In contrast to this increase, the signals in air and in the aorta declined. Nevertheless, the overall image quality still increased. This phenomenon can be explained by the proportions of signal and noise being significantly more favorable toward increasing SNR values. In contrast to the increased SNR, the CNR exhibited a statistically non-significant increase with the use of IR and the ICD assembly (CNR aorta: $P < 0.062$ and CNR in air: $P < 0.069$).

The positive effects of the iterative algorithms can clearly be affirmed, compared to FBP. Regarding the use of the ICD and iteration, one possible gain was the further beneficial radiation minimization, along with enhanced image quality in the low-dose imaging spectrum. The current data set provided a significant result for the improvement of image

quality, as emphasized by the SNR values in air, the aorta, and bone tissue.

Limitations

To select the distribution of our study population, we used an alternative approach in contrast to body mass index (BMI). For a better estimation of the proportions of the bodies scanned, we calculated the volume of the thorax. The study population had a normal distribution of chest volume and, as mentioned above, a comparable chest physiology. As a limitation of our results, no BMI correlation was performed. In addition, the image parameters for SNR and CNR calculations were measured on a single slice position. Multiple slice measurements would further influence SNR and CNR depending on the selected slice position. As scan volume might act as an important confounder, the scan volumes were retrospectively compared among the three subgroups investigated. Comparing the scan volumes, no statistically significant difference could be observed. Therefore, we conclude that comparison of the three investigated subgroups is justified.

CONCLUSION

Every step in technical improvements, including iteration and ICD geometry, has resulted in a significant reduction in radiation exposure, with a constant or better image quality level. In conclusion, we can state that the implementation of these recent developments, namely IR and the ICD, indicates possible further dose reduction in chest exams, without a loss of diagnostic image quality.

REFERENCES

1. Cranley K, Webb JA, Bell TK. A refinement to a radiation dose reduction modification for an EMI CT 5005 whole body scanner filtration system. Br J Radiol 1983;56:770-2.
2. Moran PR, Perman WH, Brown RL. Order-of-magnitude dose reduction for the EMI CT-5005. Med Phys 1978;5:67-8.
3. Kalender WA, Seissler W, Klotz E, Vock P. Spiral volumetric CT with single-breath-hold technique, continuous transport, and continuous scanner rotation. Radiology 1990;176:181-3.
4. Pesenti Rossi D, Fargetas S, Georges JL, Convers R, Baron N, Gibault-Genty G, et al. Low dose cardiac computed tomography: How to obtain it? Ann Cardiol Angeiol (Paris) 2012;61:357-64.
5. Kalender WA, Wolf H, Suess C. Dose reduction in CT by anatomically adapted tube current modulation. II. Phantom measurements. Med Phys 1999;26:2248-53.
6. Kalra MK, Maher MM, Toth TL, Schmidt B, Westerman BL, Morgan HT, et al. Techniques and applications of automatic tube current modulation for CT. Radiology 2004;233:649-57.
7. Graser A, Wintersperger BJ, Suess C, Reiser MF, Becker CR. Dose reduction and image quality in MDCT colonography using tube current modulation. AJR Am J Roentgenol 2006;187:695-701.
8. Greess H, Wolf H, Baum U, Lell M, Pirkl M, Kalender W, et al. Dose reduction in computed tomography by attenuation-based on-line

modulation of tube current: Evaluation of six anatomical regions. Eur Radiol 2000;10:391-4.

9. Kojima H, Tsujimura A, Yabe H. Usefulness of the adaptive dose shield for the infant CT. Nihon Hoshasen Gijutsu Gakkai Zasshi 2011;67:57-61.

10. Hein E, Rogalla P, Klingebiel R, Hamm B. Low-dose CT of the paranasal sinuses with eye lens protection: Effect on image quality and radiation dose. Eur Radiol 2002;12:1693-6.

11. Hopper KD, King SH, Lobell ME, TenHave TR, Weaver JS. The breast: In-plane x-ray protection during diagnostic thoracic CT-shielding with bismuth radioprotective garments. Radiology 1997;205:853-8.

12. Hopper KD. Orbital, thyroid, and breast superficial radiation shielding for patients undergoing diagnostic CT. Semin Ultrasound CT MR 2002;23:423-7.

13. Hopper KD, Neuman JD, King SH, Kunselman AR. Radioprotection to the eye during CT scanning. AJNR Am J Neuroradiol 2001;22:1194-8.

14. McLaughlin DJ, Mooney RB. Dose reduction to radiosensitive tissues in CT. Do commercially available shields meet the users' needs? Clin Radiol 2004;59:446-50.

15. Prakash P, Kalra MK, Digumarthy SR, Hsieh J, Pien H, Singh S, et al. Radiation dose reduction with chest computed tomography using adaptive statistical iterative reconstruction technique: Initial experience. J Comput Assist Tomogr 2010;34:40-5.

16. Pontana F, Duhamel A, Pagniez J, Flohr T, Faivre JB, Hachulla AL, et al. Chest computed tomography using iterative reconstruction vs filtered back projection (Part 2): Image quality of low-dose CT examinations in 80 patients. Eur Radiol 2011;21:636-43.

17. Ulzheimer S. Stellar detector performance in computed tomography: The first fully-integrated detector in the CT industry sets a new reference in image quality with HiDynamics, TrueSignal and Ultra Fast Ceramics. Somatom Sessions, Siemens 2011;29:64-6.

18. Seeram E. Computed Tomography: Physical Principles, Clinical Applications and Quality Control. Philadelphia, PA: WB Saunders Company; 1994. p. pp 1-16

19. Goldman LW. Principles of CT: Radiation dose and image quality. J Nucl Med Technol 2007;35:213-28.

20. Stoyanov D, Vassileva J. Influence of exposure parameters on patient dose and image noise in computed tomography. Pol J Med Phys Eng 2009;15:215-26.

21. Christe A, Lin MC, Yen AC, Hallett RL, Roychoudhury K, Schmitzberger F, et al. CT patterns of fungal pulmonary infections of the lung: Comparison of standard-dose and simulated low-dose CT. Eur J Radiol 2011;81:2860-6.

22. Winklehner A, Karlo C, Puippe G, Schmidt B, Flohr T, Goetti R, et al. Raw data-based iterative reconstruction in body CTA: Evaluation of radiation dose saving potential. Eur Radiol 2011;21:2521-6.

23. Kalra MK, Woisetschläger M, Dahlström N, Singh S, Digumarthy S, Do S, et al. Sinogram-affirmed iterative reconstruction of low-dose chest CT: Effect on image quality and radiation dose. AJR Am J Roentgenol 2013;201:W235-44.

24. Zar JH. Biostatistical Analysis. 5ᵗʰ ed. Upper Saddle River, NJ: Pearson, Prentice-Hall; 2010. p. 543-555.

25. Willemink MJ, de Jong PA, Leiner T, de Heer LM, Nievelstein RA, Budde RP, et al. Iterative reconstruction techniques for computed tomography part 1: Technical principles. Eur Radiol 2013;23:1623-31.

26. Willemink MJ, Leiner T, de Jong PA, de Heer LM, Nievelstein RA, Schilham AM, et al. Iterative reconstruction techniques for computed tomography part 2: Initial results in dose reduction and image quality. Eur Radiol 2013;23:1632-42.

27. Christe A, Heverhagen J, Ozdoba C, Weisstanner C, Ulzheimer S, Ebner L. CT dose and image quality in the last three scanner generations. World J Radiol 2013;5:421-9.

28. Beekma FJ, Kamphuis C. Ordered subset reconstruction for x-ray CT. Phys Med Biol 2001;46:1835-44.

29. Christe A, Charimo-Torrente J, Roychoudhury K, Vock P, Roos JE. Accuracy of low-dose computed tomography (CT) for detecting and characterizing the most common CT-patterns of pulmonary disease. Eur J Radiol 2013;82:e142-50.

30. Kalra MK, Woisetschläger M, Dahlström N, Singh S, Lindblom M, Choy G, et al. Radiation dose reduction with sinogram affirmed iterative reconstruction technique for abdominal computed tomography. J Comput Assist Tomogr 2012;36:339-46.